American Mineralogist, Volume 85, pages 1053–1060, 2000

$^{VIII}(Mg,Fe)_{0.85}{}^{VI}(Mg,Fe)_4{}^{IV}(Fe,Ge)_3O_{12}$: A new tetragonal phase and its comparison with garnet

DAVID LÉVY AND JACQUES BARBIER*

Department of Chemistry, McMaster University, Hamilton, Ontario, L8S 4M1, Canada

ABSTRACT

Tetragonal $Mg_{2.12}Fe_{3.17}Ge_{2.56}O_{12}$ is a new germanate forming at 1 atm pressure in the MgO-Fe_2O_3-GeO_2 system. It is an analogue of the high-pressure silicate mineral TAPP occurring as inclusions in diamonds of lower-mantle origin. Its crystal structure was determined by X-ray diffraction using single-crystals grown from a potassium molybdate flux. It crystallizes in the $I\bar{4}2d$ space group with a = 6.8153(4) Å, c = 18.669(2) Å, Z = 4. The refinement of its cation distribution, $^{VIII}(Mg_{0.52}Fe_{0.33})^{VI}(Mg_{1.60}Fe_{2.40})^{IV}(Ge_{2.56}Fe_{0.44})O_{12}$, shows the presence of a partially filled (85%) dodecahedral site characterized by an unusual geometry with two very different bond lengths [2.169 Å (×4) and 2.609 Å (×4)]. The structure determinations of the Ca^{2+}- and Y^{3+}-substituted phases show that the larger cations are completely partitioned in the dodecahedral site, increasing its occupancy slightly (up to 92% in the case of Ca^{2+}).

Cubic $Mg_{2.35}Y_{2.00}Fe_{0.97}Ge_{2.59}O_{12}$ is a new garnet phase forming at 1 atm pressure in the MgO-Y_2O_3-Fe_2O_3-GeO_2 system. Its crystal structure and cation distribution were also determined by single-crystal X-ray diffraction: $^{VIII}(MgY_2)^{VI}(Mg_{1.35}Fe_{0.56})^{IV}(Ge_{2.59}Fe_{0.41})O_{12}$, $Ia\bar{3}d$ space group, a = 12.232(1) Å, Z = 8. In spite of similarities in their chemical compositions, the tetragonal and garnet phases are structurally distinct, with different ratios of dodecahedral to octahedral sites, viz., $^{VIII}A^{VI}B_4{}^{IV}T_3O_{12}$ and $^{VIII}A_3{}^{VI}B_2{}^{IV}T_3O_{12}$ respectively. As a consequence, the tetragonal phase forms in systems containing smaller cations, such as Mg^{2+}, Fe^{3+}, Ni^{2+}, Co^{2+}, whereas larger cations, such as Y^{3+}, show a strong preference for the garnet phase.

INTRODUCTION

During investigation of the MgO-Fe_2O_3-GeO_2 system at 1 atm pressure (Fig. 1), a new tetragonal phase, $Mg_{2.12}Fe_{3.17}Ge_{2.56}O_{12}$, was initially synthesized in microcrystalline form (Maïssa 1994, unpublished). This new germanate phase is an analogue of the silicate mineral identified as TAPP (tetragonal almandine pyrope phase) and recently discovered as inclusions in lower-mantle diamonds (Harris et al. 1997). Based on the chemical composition, viz. $Ca_{0.01}Na_{0.02}Mg_{2.73}Fe^{2+}_{0.08}Mn^{2+}_{0.03}Al_{1.90}Fe^{3+}_{0.19}Cr^{3+}_{0.12}Si_{2.92}O_{12}$ or $A^{2+}_{2.84}B^{3+}_{2.21}Si_{2.92}O_{12}$ for sample 206B (Harris et al. 1997), TAPP shows a strong similarity with garnet but is structurally distinct from it and represents a new structure-type for silicates (Harris et al. 1997). However, TAPP has in fact several synthetic inorganic analogues that had been characterized previously. These include the $M_{4.5}As_3O_{12}$ arsenates (originally formulated as $M_3As_2O_8$) with M = Mg (Krishnamachari and Calvo 1973) and M = Co (Gopal et al. 1980), the $NaMg_4V_3O_{12}$ and $Li_{6x}Mg_{4.5-3x}V_3O_{12}$ ($0.1<x<0.15$) vanadates (Murashova et al. 1988; Torres-Trevino et al. 1986), and the $Fe_{5.33}Ge_{2.67}O_{12}$ iron germanate (originally formulated as $Fe_4Ge_2O_9$) in the FeO-Fe_2O_3-GeO_2 system (Takayama et al. 1981; Moderassi et al. 1984). Interestingly, no analogue of the tetragonal phase has been identified at 1atm pressure in the MgO-Ga_2O_3-GeO_2 system (Barbier 1998).

The present paper describes the structure of the tetragonal phase in the MgO-Fe_2O_3-GeO_2 system with a particular emphasis on its cation distribution and its comparison with the distributions in other isostructural phases. Of particular interest is the presence in the tetragonal phase of a partially filled dodecahedral site with a variable occupancy ranging from 50% in the $M_{4.5}As_3O_{12}$ arsenates to 95–100% in TAPP (Tables 1 and 2 of Harris et al. 1997). As discussed below, the full occupancy of this site in the tetragonal vanadates and iron germanate, as implied by their stoichiometries, remains in doubt. To investigate the crystal chemistry of the tetragonal phase further, Ca- and Y-substituted phases were also synthesized in single crystal form and structurally refined. A crystal chemical comparison is made between the tetragonal and garnet structures, based on the structure determination of a new garnet phase synthesized at 1 atm pressure in the MgO-Fe_2O_3-Y_2O_3-GeO_2 system.

EXPERIMENTAL METHODS

Synthesis of compounds

Single-crystals of the new tetragonal phase were obtained by the flux growth method from a powder sample with the composition $Mg_{0.84}Fe_{3.34}Ge_{3.14}O_{12}$ and $K_2Mo_2O_7$ as a flux. Oxide powders were prereacted at 1125 °C for 3 days with daily regrinding. The sample-flux mixture, with a 5:4 g ratio, was melted at 1325 °C in a covered Pt crucible, kept at that temperature for 12 hours, cooled at 3 °C·h^{-1} to a final temperature

*E-mail: barbier@mcmaster.ca

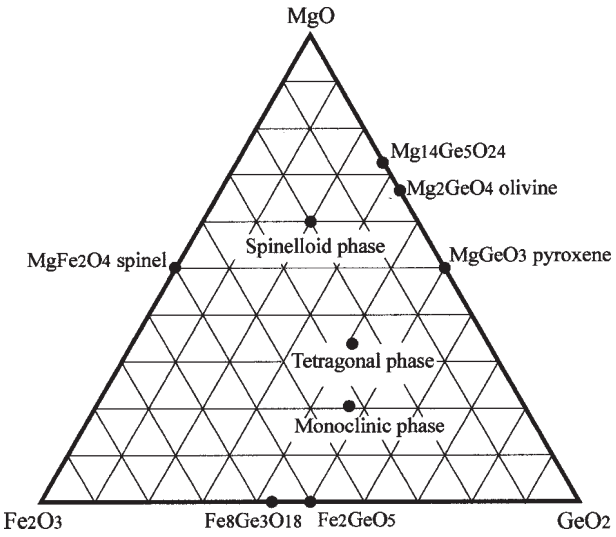

FIGURE 1. Schematic diagram of the MgO-Fe_2O_3-GeO_2 system showing the known binary and ternary phases at P = 1 atm and T = 1000–1200 °C. The compositions of the tetragonal phase, $Mg_{2.12}Fe_{3.17}Ge_{2.56}O_{12}$ (this work), and of the monoclinic phase, $Mg_{0.77}Fe_{2.45}Ge_{1.78}O_8$ (Lévy and Barbier unpublished manuscript), were determined by electron microprobe analysis of flux-grown single-crystals. The nominal composition of the spinelloid phase III, $Mg_3Fe_2GeO_8$, was determined by powder X-ray diffraction (Barbier 1989).

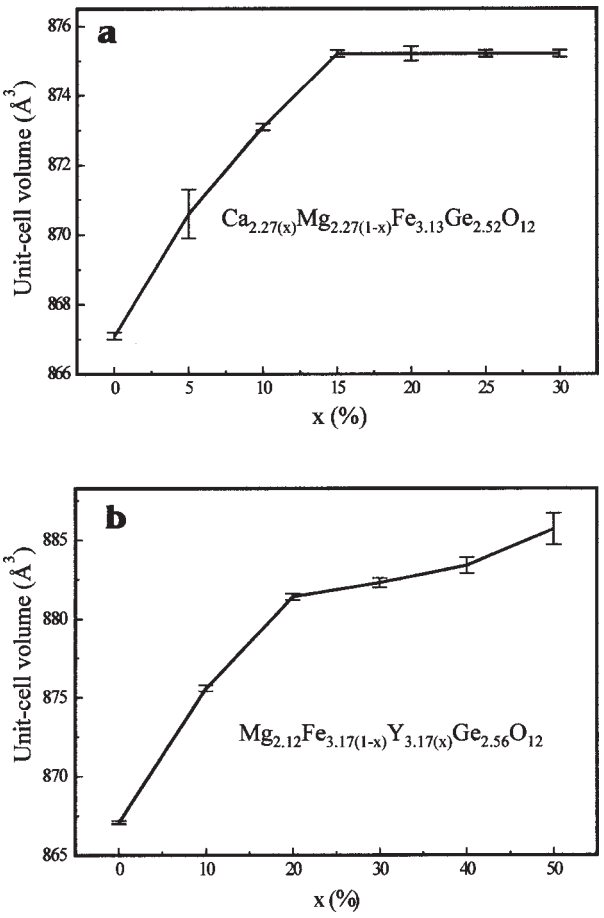

FIGURE 2. Variation of the unit-cell volumes of the Ca- and Y-substituted tetragonal phases as a function of Ca-content (**a**) and Y-content (**b**). The error bars correspond to the standard deviations calculated during the least-squares refinement of the unit-cell parameters from powder X-ray data.

of 1200 °C and then air-quenched. The flux was dissolved in hot water and the recovered product consisted of thin plates of α-Fe_2O_3 and brown truncated pyramidal crystals of the tetragonal phase. The composition of the latter, $Mg_{2.12}Fe_{3.17}Ge_{2.56}O_{12}$, was determined by electron microprobe analysis (Table 1) using single-crystals of Mg_2GeO_4 olivine and $Ca_3Fe_2Ge_3O_{12}$ garnet as standards.

As shown by the microprobe analysis, the tetragonal phase contains only 7.85 cations for 12 oxygen atoms, corresponding to a structural formula of $^{VIII}(Mg,Fe)_{0.85}{}^{VI}(Mg,Fe)_4{}^{IV}(Ge,Fe)_3O_{12}$ with a partially filled dodecahedral site (see below). To determine if this cation deficiency could be reduced by introducing larger ions, two solid solutions based on Ca^{2+}/Mg^{2+} and Y^{3+}/Fe^{3+} substitutions were studied. Six samples with compositions $Ca_{2.27(x)}Mg_{2.27(1-x)}Fe_{3.13}Ge_{2.52}O_{12}$ (x = 5, 10, 15, 20, 25, and 30%) were prepared by solid-state reaction at 1200 °C. As expected, the unit-cell volume increases as the calcium content increases up to x = 15% indicating the formation of a limited Ca^{2+} = Mg^{2+} solid solution (Fig. 2a). For samples with x = 20, 25, and 30%, the presence of impurity lines in the powder patterns indicated clearly that the limit of the solid solution had been exceeded. Five other samples with compositions $Mg_{2.12}Fe_{3.17(1-x)}Y_{3.17(x)}Ge_{2.52}O_{12}$ (x = 10, 20, 30, 40, and 50%) were also prepared under the same conditions. In this case, the unit-cell volume increases up to 20% due to the formation of a $Y^{3+} = Fe^{3+}$ solid solution (Fig. 2b). The further small increase from x = 20 to 50% possibly corresponds to a different substitution, i.e., Mg^{2+}

TABLE 1. Electron microprobe analyses (wt%) of the tetragonal and garnet phases

Phase	CaO	Fe_2O_3	GeO_2	MgO	Y_2O_3	Total	No. of analyses
$Mg_{2.12}Fe_{3.17}Ge_{2.56}O_{12}$	–	41.35(13)	43.87(46)	14.00(14)	–	99.23	8
$Ca_{0.32}Mg_{1.94}Fe_{3.12}Ge_{2.52}O_{12}$	2.96(1)	40.69(27)	42.85(42)	12.76(9)	–	99.26	8
$Mg_{1.76}Fe_{3.37}Y_{0.68}Ge_{2.08}O_{12}$	–	41.85(99)	33.78(92)	11.06(51)	12.01(34)	98.70	6
$Mg_{2.35}Y_{2.00}Fe_{0.97}Ge_{2.59}O_{12}$*	–	11.56(1)	40.34(87)	14.07(19)	33.64(87)	99.61	3

Note: The numbers in parentheses are the e.s.d.s calculated from the individual analyses of each phase.
* Garnet structure.

+ Ge^{4+} = $2Fe^{3+}$, which is suggested by electron microprobe analyses of flux-grown single-crystals (Table 1).

The same growth conditions were used to obtain single-crystals of the Ca-substituted tetragonal phase. The nutrient consisted of unreacted carbonate and oxide powders with a nominal composition of $Ca_{1.14}Mg_{1.13}Fe_{3.13}Ge_{2.52}O_{12}$, with a much higher Ca-content than the solid-solution limit in order to ensure that the crystals would be saturated in calcium. The recovered product consisted again of brown truncated pyramidal crystals similar in shape and size to the crystals of the Ca-free phase. Their average $Ca_{0.32}Mg_{1.94}Fe_{3.12}Ge_{2.52}O_{12}$ composition (Table 1) is similar to that of the Ca-free phase and their $Ca^{2+}/(Ca^{2+}+Mg^{2+})$ ratio of 14.5% corresponds indeed to the limit of the $Ca^{2+} = Mg^{2+}$ solid solution.

In the case of the Y-substituted tetragonal phase, the nutrient for the crystal growth had an yttrium-rich composition of $Mg_{2.12}Fe_{1.58}Y_{1.58}Ge_{2.52}O_{12}$ formed of the unreacted MgO, Fe_2O_3, Y_2O_3 and GeO_2 oxides. The recovered product included brown truncated pyramidal crystals of tetragonal $Mg_{1.76}Y_{0.68}Fe_{3.37}Ge_{2.08}O_{12}$ together with colorless crystals of $Y_2Ge_2O_7$ and orange crystals of a garnet phase with composition $Mg_{2.35}Y_{2.00}Fe_{0.97}Ge_{2.59}O_{12}$. The $Y_2Ge_2O_7$ crystals were used as the yttrium standard for the electron microprobe analyses (Table 1).

Structure determinations

The X-ray data collections were performed at McMaster University with a P4 Siemens diffractometer equipped with a Siemens SMART 1K charge-couple device (CCD) area detector and a rotating anode using graphite-monochromated Mo$K\alpha$ radiation. The data collection and processing were carried out by use of the program SAINT (Siemens 1996) that applied Lorentz and polarization corrections to three-dimensionally integrated diffraction spots. The program SADABS (Sheldrick 1996) was used for the scaling of the diffraction data and to perform empirical absorption corrections based on redundant reflections. Details of the structure determinations with the SHELXL97 software (Shledrick 1997) are summarized in Table 2.

The structure of tetragonal $Mg_{2.12}Fe_{3.17}Ge_{2.56}O_{12}$ was determined by direct methods and Fourier difference maps that located the five metal sites and the three oxygen sites. Two of the metal sites (T1 and T2) have a tetrahedral environment and were assigned to Ge atoms. However these sites correspond to the 4b and 8d positions of the $I\bar{4}2d$ space group and, if totally filled by Ge, would give 12 Ge atoms per unit cell. The lower Ge-content shown by the microprobe analysis, i.e., $Mg_{8.48}Fe_{12.68}Ge_{10.24}O_{48}$, led to the conclusion that the tetrahedral sites also contain Fe. Average bond distances (1.745 vs. 1.777 Å) and bond-valence sums (4.04 vs. 3.70, calculated using the parameters of Brese and O'Keeffe 1991) for the T1 and T2 sites respectively indicated that T1 contained Ge only, whereas T2 contained 21.75% Fe^{3+} as calculated from the chemical composition, viz., $Mg_{8.48}Fe_{10.92}{}^{IV}Ge_4{}^{IV}(Fe_{1.76}Ge_{6.24})O_{48}$. The remaining three metal sites correspond to one dodecahedron (M1, or A by analogy with the garnet structure) and two octahedra (M2 and M3) in the 4a, 8d and 8c positions, respectively. Only 19.40 cations (8.48 Mg + 10.92 Fe) were available to fill these sites implying the presence of vacancies that were introduced on the dodecahedral M1 site as suggested by a higher isotropic displacement parameter (0.0190 vs. 0.0100 and 0.0087 Å^2). The occupancy of the dodecahedral site was therefore calculated to be (20–19.40)/4 = 85%. All three M1, M2, and M3 sites contained mixed Mg+Fe occupancies that were refined by constraining the total Mg- and Fe-contents of the unit-cell according to the composition given by the microprobe analysis. The scattering factors for neutral atoms contained in the SHELXL software were used for the refinement, together with a refinable occupancy factor for each site. After convergence, the site populations yielded a structural formula of $^{VIII}(Mg_{0.52}Fe_{0.33})^{VI}(Mg_{1.60}Fe_{2.40})^{IV}(Ge_{2.56}Fe_{0.44})O_{12}$.

The atomic coordinates determined for $Mg_{2.12}Fe_{3.17}Ge_{2.56}O_{12}$ were used as a starting point for the structure refinement of the Ca-substituted tetragonal phase since the only difference be-

TABLE 2. Crystal data and details of the structure refinements for the tetragonal and garnet phases

Phase	$Mg_{2.12}Fe_{3.17}Ge_{2.56}O_{12}$	$Mg_{1.95}Ca_{0.33}Fe_{3.13}Ge_{2.52}O_{12}$	$Mg_{1.76}Fe_{3.37}Y_{0.68}Ge_{2.08}O_{12}$	$Mg_{2.35}Y_{2.00}Fe_{0.97}Ge_{2.59}O_{12}$
Crystal size (mm)	0.3 × 0.2 × 0.2	0.3 × 0.15 × 0.07	0.09 × 0.08 × 0.06	0.10 × 0.10 × 0.10
Space group	$I\bar{4}2d$	$I\bar{4}2d$	$I\bar{4}2d$	$Ia\bar{3}d$
Unit cell (Å)*	a = 6.8153(4) c = 18.669(2)	a = 6.8217(5) c = 18.782(2)	a = 6.8290(9) c = 18.994(5)	a = 12.232(1)
Volume (Å^3)	867.1	874.0	885.8	1830.0
Z	4	4	4	8
Calc. density (g/cm^3)	4.645	4.639	4.757	4.857
Wavelength (Å)	0.71073	0.71073	0.71073	0.71073
Absorption coeff. (mm^{-1})	14.244	13.922	16.980	22.779
θ range (°)	3.18–38.63	3.18–38.81	3.17–36.61	4.08–36.54
Index ranges	–8 ≤ h ≤ 11 –10 ≤ k ≤ 11 –27 ≤ l ≤ 32	–11 ≤ h ≤ 10 –10 ≤ k ≤ 11 –24 ≤ l ≤ 32	–11 ≤ h ≤ 10 –6 ≤ k ≤ 11 –17 ≤ l ≤ 31	–8 ≤ h ≤ 20 –15 ≤ k ≤ 20 –20 ≤ l ≤ 18
Unique reflections	1158	1166	1028	378
T_{min}, T_{max}	0.0279, 0.0964	0.0960, 0.1883	0.2495, 0.3462	0.1823,0.2369
R_{int}	0.044	0.043	0.038	0.088
Refined parameters	51	51	51	18
Goodness-of-fit	1.149	1.077	1.085	1.047
$R[F>4s(F)]$	0.0254	0.0241	0.0384	0.035
$wR(F^2)$	0.0633	0.0591	0.0891	0.088
Difference map (e/Å^3)	1.686 –1.361	1.213 –1.375	2.027 –1.777	0.675 –0.860

Notes: The SADABS absorption correction and a full matrix least-square refinement method on F^2 were used for all cases.
* The unit-cell dimensions have been measured by powder X-ray diffraction using crushed single crystals (Guinier camera with Fe$K\alpha_1$ radiation and Y_2O_3 as internal standard).

tween the two compounds is a 14.5% substitution of Ca^{2+} for Mg^{2+}. However, during the refinement it appeared that the crystal selected for data collection corresponded to an inverted structure, resulting in opposite signs for the *y* atomic coordinates (Table 3). The T1 site remained filled with Ge only in agreement with the <T1-O> distance (1.743Å) and the bond-valence sum (4.05). The population of the T2 site was fixed at (76% Ge^{4+} + 24% Fe^{3+}) as calculated from the chemical composition, $Ca_{1.28}Mg_{7.80}Fe_{10.64}{}^{IV}Ge_4{}^{IV}(Fe_{1.92}Ge_{6.08})O_{48}$. Only 19.62 cations were available to fill the M1, M2 and M3 sites that again indicated vacancies on the M1 site with an occupancy of 92%. Initially, mixed Fe+Mg+Ca occupancies were introduced on all M sites and refined by constraining the total Ca, Mg and Fe contents. After a few cycles, however, the Ca-contents of the M2 and M3 sites had converged to zero indicating that all Ca was located on the M1 dodecahedral site. The mixed Mg+Fe occupancies were then further refined by constraining the total Mg- and Fe-contents. The final site occupancies correspond to a structural formula of $^{VIII}(Ca_{0.32}Mg_{0.42}Fe_{0.18})^{VI}(Mg_{1.53}Fe_{2.47})^{IV}(Ge_{2.52}Fe_{0.48})O_{12}$.

TABLE 3. Atomic coordinates, site occupancies and equivalent isotropic displacement parameters for the tetragonal and garnet phases

Atom	*x*	*y*	*z*	U_{eq} (Å^2)
		Tetragonal $Mg_{2.12}Fe_{3.17}Ge_{2.56}O_{12}$ *		
T1	1/2	1/2	0	0.0099(1)
T2	–0.16216(6)	1/4	1/8	0.0110(1)
M1	0	0	0	0.0191(4)
M2	0.2564(1)	1/4	1/8	0.0100(1)
M3	0	1/2	–0.02186(4)	0.0087(2)
O1	0.0137(3)	0.2815(3)	0.0540(1)	0.0132(4)
O2	–0.2708(4)	0.0285(3)	0.0983(1)	0.0179(4)
O3	0.4500(4)	0.2836(3)	0.0464(1)	0.0163(4)
		Tetragonal $Mg_{1.95}Ca_{0.32}Fe_{3.13}Ge_{2.52}O_{12}$†		
T1	1/2	1/2	0	0.0097(1)
T2	–0.16313(6)	–1/4	1/8	0.0111(1)
M1	0	0	0	0.0143(3)
M2	0.25705(9)	–1/4	1/8	0.0103(3)
M3	0	1/2	–0.02129(4)	0.0088(2)
O1	0.0138(3)	–0.2870(3)	0.05521(9)	0.0153(4)
O2	–0.2690(3)	–0.0288(3)	0.0965(1)	0.0173(4)
O3	0.4500(3)	–0.2846(3)	0.0464(1)	0.0159(4)
		Tetragonal $Mg_{1.76}Y_{0.68}Fe_{3.37}Ge_{2.08}O_{12}$‡		
T1	1/2	1/2	0	0.0118(2)
T2	–0.1654(2)	1/4	1/8	0.0151(2)
M1	0	0	0	0.0125(2)
M2	0.2559(2)	1/4	1/8	0.0131(3)
M3	0	1/2	–0.02037(7)	0.0107(3)
O1	0.0116(6)	0.2896(5)	0.0555(2)	0.0149(7)
O2	–0.2615(6)	0.0246(5)	0.0936(2)	0.0201(7)
O3	0.4577(7)	0.2863(5)	0.0480(2)	0.0220(9)
		Cubic $Mg_{2.35}Y_{2.00}Fe_{0.97}Ge_{2.59}O_{12}$§		
T	0	1/4	3/8	0.0089(3)
A	0	1/4	1/8	0.0110(3)
M	0	0	0	0.0118(4)
O	–0.0308(2)	0.0555(2)	0.1555(2)	0.0130(6)

* T1 = Ge, T2 = 0.783 Ge + 0.217 Fe, M1 = 0.331(8) Fe + 0.522(8) Mg, M2 = 0.782(2) Fe + 0.218(2) Mg, M3 = 0.437(2) Fe + 0.563(2) Mg.
† T1 = Ge, T2 = 0.759 Ge + 0.241 Fe, M1= 0.179(3) Fe + 0.413(3) Mg + 0.325 Ca, M2 = 0.755(2) Fe + 0.245(2) Mg, M3 = 0.478(2) Fe + 0.522(2) Mg.
‡ T1 = Ge, T2 = 0.538 Ge + 0.462 Fe, M1= 0.684 Y + 0.212 Mg, M2 = 0.738(5) Fe + 0.262(5) Mg, M3 = 0.485(5) Fe + 0.515(5) Mg.
§ T = 0.865 Ge + 0.135 Fe, A = 0.667 Y + 0.333 Mg, M = 0.284 Fe + 0.675 Mg.

The same refinement procedure was also used for the Y-substituted tetragonal phase. The <T1-O> distance (1.745 Å) and the bond-valence sum (4.03) were again in agreement with an occupancy of 100% Ge for the T1 site. The population of the T2 site was fixed at (43.8% Ge + 46.2% Fe) according to the chemical composition $Mg_{7.06}Fe_{9.79}Y_{2.72}{}^{IV}Ge_4{}^{IV}(Fe_{3.69}Ge_{4.31})O_{48}$. The total number of M cations (19.57) also resulted in a partial occupancy of the M1 site equal to 89%. Initially, mixed Fe+Mg+Y occupancies were introduced on the M1, M2 and M3 sites but the Y-content of the M2 and M3 sites converged to zero as well as the Fe-content of the M1 site. This led to an occupancy of 58% Y and 31% Mg for the M1 site while the M2 and M3 sites contained mixed Mg+Fe populations that were further refined by constraining the total Mg- and Fe-contents. The resulting structural formula is $^{VIII}(Y_{0.68}Mg_{0.21})^{VI}(Mg_{1.55}Fe_{2.45})^{IV}(Ge_{2.08}Fe_{0.92})O_{12}$. For this particular phase, the refinement included the presence of a chiral twin with a 51(2)% volume fraction.

The final atomic coordinates and site occupancies for all three tetragonal phases are listed in Table 3 and the anisotropic displacement parameters are given in Table 4. Selected bond distances are shown in Table 5.

The structure of the $Mg_{2.35}Y_{2.00}Fe_{0.97}Ge_{2.59}O_{12}$ garnet phase was also determined by direct methods and Fourier difference maps. The structure contains mixed occupancies for all sites, including the dodecahedral A site, the octahedral M site and the tetrahedral T site. The population of the latter was fixed at (86.4% Ge^{4+} + 13.6% Fe^{3+}) as calculated from the chemical composition of $Mg_{2.35}Y_2Fe_{0.56}{}^{IV}(Ge_{2.59}Fe_{0.41})O_{12}$. The Y^{3+} cations were constrained to occupy the dodecahedral site in agreement with their large ionic radius and with the cation distribution determined for a related garnet phase, $^{VIII}(MgY_2)^{VI}Mg_2{}^{IV}Ge_3O_{12}$ (Lévy and Barbier 1999). The slightly cation-deficient composition, $M_{4.91}T_3O_{12}$, given by the electron microprobe analysis could be accounted for by introducing vacancies either on the dodecahedral site or on the octahedral site. It was found that the octahedral vacancy model led to slightly better agreement factors and a cleaner electron density difference map [$wR(F^2) = 0.0888$, $(\Delta\rho)_{max} = 0.67$e/Å^3 and $(\Delta\rho)_{min} = -0.86$e/Å^3 vs. 0.0917, 0.74, and –1.39, respectively]. The corresponding structural formula is $^{VIII}(MgY_2)^{VI}(Mg_{1.35}Fe_{0.56})^{IV}(Ge_{2.59}Fe_{0.41})O_{12}$ with a 9% cation-deficiency on the octahedral site. The final atomic coordinates and site occupancies are listed in Table 3, the anisotropic displacement parameters are listed in Table 4 and selected bond distances are given in Table 6. Although octahedral vacancies are uncommon in garnet structures, an even larger octahedral deficiency has previously been reported in the structure of $^{VIII}(Ca_{2.5}Mg_{0.5})^{VI}(Mg_{0.75}Cu_{0.75})^{IV}V_3O_{12}$ (Vogt and Müller-Buschbaum 1991).

DESCRIPTION OF THE TETRAGONAL STRUCTURE

The three tetragonal phases are isostructural and, therefore, only the structure of the $Mg_{2.12}Fe_{3.17}Ge_{2.56}O_{12}$ phase will be described here.

Unlike the two other ternary compounds so far identified in the MgO-Fe_2O_3-GeO_2 system, namely monoclinic $^{VI}(Mg_{0.77}Fe_{2.23})^{IV}(Ge_{1.78}Fe_{0.22})O_8$ (Lévy and Barbier in preparation) and the spinelloid phase $^{VI}(Mg_3Fe)^{IV}(FeGe)O_8$ (Barbier

TABLE 4. Anisotropic displacement parameters (Å^2) for the tetragonal and garnet phases

Atom	U_{11}	U_{22}	U_{33}	U_{23}	U_{13}	U_{12}
			Tetragonal $Mg_{2.12}Fe_{3.17}Ge_{2.56}O_{12}$			
T1	0.0086(1)	0.0086(1)	0.0123(2)	0	0	0
T2	0.0147(2)	0.0075(2)	0.0106(2)	–0.0003(1)	0	0
M1	0.0114(5)	0.0114(5)	0.0344(9)	0	0	0
M2	0.0124(2)	0.0072(2)	0.0103(3)	–0.0016(2)	0	0
M3	0.0067(3)	0.0091(3)	0.0103(3)	0	0	0.0000(3)
O1	0.0124(7)	0.0156(8)	0.0114(6)	0.0011(6)	0.0018(6)	–0.0007(6)
O2	0.0182(9)	0.0137(8)	0.0218(9)	0.0049(7)	–0.0075(8)	–0.0038(7)
O3	0.025(1)	0.0080(8)	0.0156(8)	0.0005(6)	0.0053(7)	0.0009(6)
			Tetragonal $Mg_{1.95}Ca_{0.33}Fe_{3.13}Ge_{2.52}O_{12}$			
T1	0.0093(1)	0.0093(1)	0.0104(2)	0	0	0
T2	0.0157(2)	0.0082(2)	0.0094(1)	0.0000(1)	0	0
M1	0.0111(4)	0.0111(4)	0.0205(6)	0	0	0
M2	0.0132(2)	0.0083(2)	0.0093(2)	–0.0013(2)	0	0
M3	0.0075(3)	0.0096(3)	0.0094(3)	0	0	0.0002(3)
O1	0.0128(7)	0.0205(9)	0.0126(6)	–0.0041(6)	0.0020(6)	0.0004(7)
O2	0.0183(9)	0.0140(8)	0.0195(8)	0.0050(6)	0.0064(7)	0.0038(7)
O3	0.0244(9)	0.0096(8)	0.0136(7)	–0.0012(6)	0.0056(6)	–0.0004(6)
			Tetragonal $Mg_{1.76}Fe_{3.37}Y_{0.68}Ge_{2.08}O_{12}$			
T1	0.0124(3)	0.0124(3)	0.0104(4)	0	0	0
T2	0.0270(5)	0.0089(3)	0.0093(3)	–0.0002(3)	0	0
M1	0.0125(3)	0.0125(3)	0.0126(5)	0	0	0
M2	0.0195(5)	0.0099(4)	0.0098(5)	–0.0019(4)	0	0
M3	0.0096(6)	0.0104(6)	0.0120(5)	0	0	–0.0006(5)
O1	0.016(2)	0.017(2)	0.011(1)	0.004(1)	0.003(1)	0.000(1)
O2	0.020(2)	0.019(2)	0.021(2)	0.009(1)	–0.008(2)	–0.005(2)
O3	0.037(3)	0.011(2)	0.016(2)	0.000(1)	0.008(2)	–0.001(1)
			Cubic $Mg_{2.35}Y_{2.00}Fe_{0.97}Ge_{2.59}O_{12}$			
T	0.0077(3)	0.0077(3)	0.0113(5)	0	0	0
A	0.0122(3)	0.0122(3)	0.0086(5)	0	0	0
M	0.0118(4)	0.0118(4)	0.0118(4)	–0.0006(6)	–0.0006(6)	–0.0006(6)
O	0.015(1)	0.014(1)	0.010(1)	0.002(1)	0.002(1)	–0.001(1)

Note: The anisotropic displacement factor exponent takes the form: $-2\pi^2[h^2a^{*2}U_{11}+\ldots 2hka^*b^*U_{12}]$.

TABLE 5. Selected bond lengths (Å) in the tetragonal phases

	$Mg_{2.12}Fe_{3.17}Ge_{2.56}O_{12}$	$Mg_{1.95}Ca_{0.33}Fe_{3.13}Ge_{2.52}O_{12}$	$Mg_{1.76}Fe_{3.37}Y_{0.68}Ge_{2.08}O_{12}$
T1-O3 ×4	1.745(2)	1.743(2)	1.745(4)
T2-O2 ×2	1.754(2)	1.756(2)	1.777(4)
T2-O1 ×2	1.800(2)	1.800(2)	1.811(4)
Mean T2-O	1.777	1.778	1.794
M1-O1 ×4	2.169(2)	2.218(2)	2.243(4)
M1-O2 ×4	2.609(2)	2.587(2)	2.526(4)
Mean M1-O	2.389	2.403	2.384
M2-O2 ×2	1.965(2)	1.978(2)	1.968(4)
M2-O3 ×2	1.986(2)	1.991(2)	2.024(4)
M2-O1 ×2	2.130(2)	2.130(0)	2.144(4)
Mean M2-O	2.027	2.033	2.045
M3-O3 ×2	2.015(2)	2.027(2)	2.036(3)
M3-O1 ×2	2.057(2)	2.045(2)	2.046(4)
M3-O2 ×2	2.124(2)	2.125(2)	2.148(4)
Mean M3-O	2.065	2.065	2.077

1989), the tetragonal structure is not based on a close-packed oxygen array. However, the volume per oxygen atom (18.1 Å^3) is almost equal to that in the spinelloid phase (18.2 Å^3) indicating that the tetragonal structure is also a dense structure. The structure (Fig. 3) is built up of tetrahedra (T1, T2), octahedra (M2, M3) and dodecahedra (M1 or A) that are connected by corner- and edge-sharing. Whereas M3 only shares corners with T1 and T2, M2 shares an edge with T2. This edge sharing leads to a smaller volume for M2 than for M3 (10.89 vs. 11.30 Å^3 respectively) that can be associated with the partial Mg/Fe or-

TABLE 6. Selected bond lengths (Å) in $Mg_{2.35}Y_{2.00}Fe_{0.97}Ge_{2.59}O_{12}$ garnet

T-O ×4	1.768(3)
A-O ×4	2.330(3)
A-O ×4	2.467(3)
Mean A-O	2.384
M-O ×6	2.054(3)

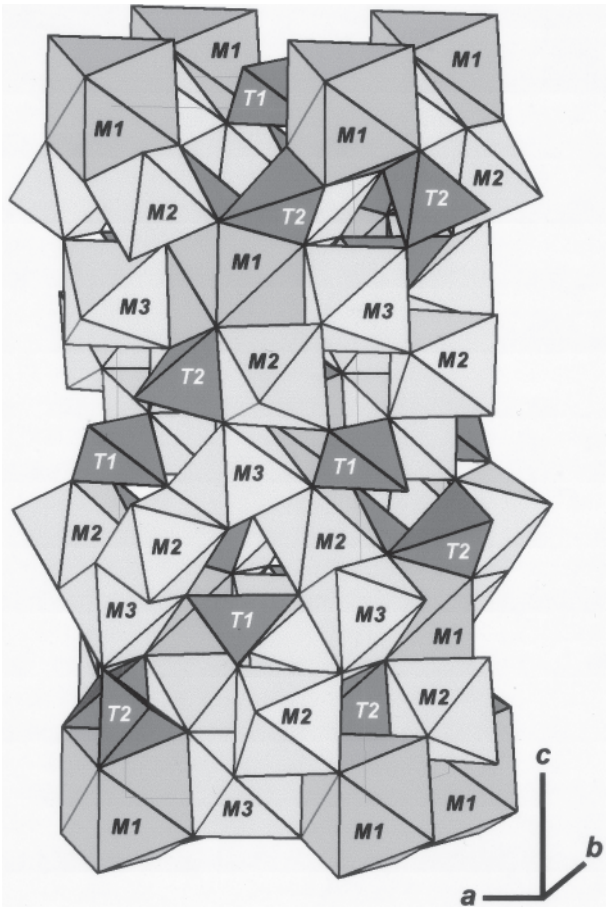

FIGURE 3. Polyhedral representation of the crystal structure of tetragonal $^{VIII}(Mg_{0.52}Fe_{0.33})^{VI}(Mg_{1.60}Fe_{2.40})^{IV}(Ge_{2.56}Fe_{0.44})O_{12}$ showing the dodecahedra (M1), octahedra (M2, M3) and tetrahedra (T1, T2). The structure contains extensive edge-sharing between M1, M2, and M3. T1 only share corners whereas T2 shares edges with M1 and M2.

dering over the two sites, with the smaller Fe^{3+} cation preferentially occupying M2 (78% Fe^{3+} + 22% Mg^{2+}) rather than M3 (44% Fe^{3+} + 56% Mg^{2+}). This edge sharing also explains the partial substitution of Ge^{4+} cations by Fe^{3+} cations on the T2 site as a way to reduce cation-cation repulsions across the shared edge. The details of the local coordination geometry, including the shortening of the shared O1-O1 edge as well as the lengthening of the T2-O1 and M2-O1 bonds, are illustrated in Figure 4. Similar structural distortions are observed in the structures of the Ca- and Y-substituted tetragonal phases.

The most remarkable feature of the tetragonal structure is the dodecahedral A site. The dodecahedra are isolated from one another but are linked by a unique pattern of edge sharing with the octahedra and tetrahedra (Fig. 3). The dodecahedra are elongated along the c-axis of the tetragonal unit-cell and their geometry is characterized by an irregular $\bar{4}$ point symmetry with four shorter A-O1 bonds (2.169 Å) and four much longer A-O2 bonds (2.609 Å). The shortening of the A-O1 bonds can be interpreted as a compensating distortion for the lenghtening of the M2-O1 and T2-O1 bonds caused by the edge sharing between T2 and M2. Overall, the average <A-O> bond is much longer than expected for either the Mg^{2+} or the Fe^{3+} cation and the resulting large site volume is reflected in the strongly anisotropic displacement of the A cation, with a large U_{33} parameter (Table 4). Interestingly, this anisotropy decreases in the Ca-substituted phase and is absent in the Y-substituted phase in which the dodecahedal sites contain 33% Ca^{2+} and 68% Y^{3+} respectively. This observation indicates that, although of unusual geometry, the dodecahedral site of the tetragonal structure is better adapted to larger cations such as Ca^{2+} and Y^{3+}, as also shown by the complete A-site partitioning of these cations. Nevertheless, the Ca^{2+} and Y^{3+} substitutions remain limited probably as a consequence of the shorter A-O1 bonds which rapidly lead to a strong overbonding around the dodecahedral cations. For instance, the A-O bond distances in the Ca-substituted phase (2.218 and 2.587 Å) yield a high bond-valence sum of 2.78 for the Ca^{2+} cations which clearly precludes a large Ca-content for the A site. A strong anisotropy was also reported for the dodecahedral (M1) site of the TAPP structure with a mixed Mg^{2+}/Fe^{3+} occupancy (Harris et al. 1997) in spite of slightly shorter bonds (2.109 and 2.521 Å) associated with the smaller unit-cell dimensions of the silicate phase.

Several previously known compounds including arsenates, vanadates and one germanate are isostructural with the present tetragonal Mg,Fe germanate and the TAPP mineral. It is of interest to compare their cation distributions and, in particular, the occupancies of their dodecahedral sites since a common feature appears to be a variable cation deficiency on this site (Table 7). The total occupancy of the dodecahedral site in TAPP (76% Mg^{2+} + 19% Fe^{3+}) is slightly larger than in the present tetragonal germanate (52% Mg^{2+} + 33% Fe^{3+}). This difference can be related to the high-pressure conditions of formation of the silicate, assuming that the greater compressibility of the A-O bonds would yield a more favourable coordination environment for the Mg^{2+} and Fe^{3+} cations at high pressure. This interpretation is supported by the observation that the A-site occupancy in the room-pressure germanate structure increases to 89% and 92% when the larger Y^{3+} and Ca^{2+} cations are present. As required by stoichiometry, the dodecahedral sites of the $M_3As_2O_8$ (M = Mg, Co) arsenates are half-filled (Krishnamachari and Calvo 1973; Gopal et al. 1980) and these compounds should be more correctly written as $M_{4.5}As_3O_{12}$ or $^{VIII}M_{0.5}{}^{VI}M_4{}^{IV}As_3O_{12}$. An even lower occupancy of 35% has been determined for the analogous Ni arsenate, $Ni_{4.35}As_3O_{11.7}(OH)_{0.3}$, synthesized under hydrothermal conditions (Barbier 1999). A full occupancy of the dodecahedral site has been reported for the vanadate $^{VIII}Na^{VI}Mg_4{}^{IV}V_3O_{12}$ (Murashova et al. 1988) that, however, has not been confirmed by a chemical analysis of the melt-grown crystals. Moreover, the Na-O bond lengths yield a rather high bond-valence sum of 1.23 that, together with a large B_{eq} parameter, suggests that some degree of Mg^{2+} = 2 Na^{+} substitution could be have taken place resulting in the formation of dodecahedral vacancies. Finally, according to the stoichiometry of the $Fe_4Ge_2O_9$ germanate, with a structural formula of $^{VIII}(Fe^{2+})^{VI}(Fe^{2+}_{1.67}Fe^{3+}_{2.33})^{IV}(Fe^{3+}_{0.33}Ge_{2.67})O_{12}$, its dodecahedral site should be 100% filled (Modaressi et al. 1984). However, an

ambiguity remains regarding the exact Fe^{2+}/Fe^{3+} ratio, and the very large B_{eq} associated with the eightfold-coordinated Fe^{2+} cation again suggests the presence of vacancies. Overall, it appears that all known tetragonal phases are likely to be cation-deficient and that they all contain vacancies on the dodecahedral site, most probably as a result of the unique and irregular geometry of this site. By contrast, the dodecahedral site in the garnet structure is typically completely filled.

COMPARISON BETWEEN THE GARNET AND TETRAGONAL STRUCTURES

Expressed in a pseudo $AO\text{-}B_2O_3\text{-}SiO_2$ system, the composition of the TAPP mineral, $A_{2.84}B_{2.21}Si_{2.92}O_{12}$, is similar to the composition of the almandine and pyrope garnets, thus explaining the acronym (Harris et al. 1997). By comparison, the tetragonal phase of the $MgO\text{-}Fe_2O_3\text{-}GeO_2$ system, $Mg_{2.12}Fe_{3.17}Ge_{2.56}O_{12}$, is much enriched in trivalent oxide via the substitution $Fe_2O_3 = MgO + GeO_2$. Although some indication has been obtained by microprobe analysis and powder X-ray diffraction (Fig. 2b) of the existence of a solid solution associated with this double substitution, no attempt has been made in this work to determine its extent more precisely. It should be noted, however, that in order to achieve an "exact" garnet stoichiometry with 8 cations for 12 O atoms, a full occupancy of the dodecahedral A site of the tetragonal structure is required. This condition is not achieved for all compositions of the TAPP mineral (e.g., the 244B sample of Harris et al. in which the refined A-site occupancy sums up to 95% only) and, as discussed above, appears not to be achieved in any of the other known tetragonal phases.

In spite of their compositional similarity, the tetragonal and garnet phases are structurally quite distinct. Both structures are built of the same types of coordination polyhedra (tetrahedra, octahedra and dodecahedra) but differ in their relative proportions as shown by their structural formulas: $^{VIII}A^{VI}B_4^{IV}T_3O_{12}$ for the tetragonal phase vs. $^{VIII}A_3^{VI}B_2^{IV}T_3O_{12}$ for garnet. The main difference lies in the ratio of octahedral (B) to dodecahedral (A) sites which, in turn, implies further differences in the octahedral/tetrahedral frameworks of the structures. In particular, the T and B sites in garnet only share corners whereas, as described earlier, one of the T sites in the tetragonal structure shares an edge with a B site (Figs. 3 and 4). The two structures also significantly differ in the geometries of their dodecahedral sites. The A site in garnet with 222 point symmetry is more regular, with a narrower spread of A-O bond lengths than the A site of the tetragonal structure with $\bar{4}$ point symmetry (Fig. 5). This difference reflects the distinct topologies of the two structures: firstly, the A sites of the tetragonal structure do not share edges with one another and are tetragonally distorted whereas the A sites of the cubic garnet structure are geometrically constrained by a more regular pattern of edge sharing, including with adjacent A sites; secondly, the absence of tetrahedral-octahedral edge sharing and the presence of a single O position in garnet result in more regular sites. The A-site in particular provides a better coordination environment for large cations as shown by the full occupancy and the more isotropic displacement of the A cations in $Ca_3Fe_2Ge_3O_8$, $Ca_3Y_2Ge_3O_8$, and $Mg_3Y_2Ge_3O_8$ (Lévy and Barbier 1999), as well as in the garnet phase of the $MgO\text{-}Fe_2O_3\text{-}Y_2O_3\text{-}GeO_2$ system (Table 4).

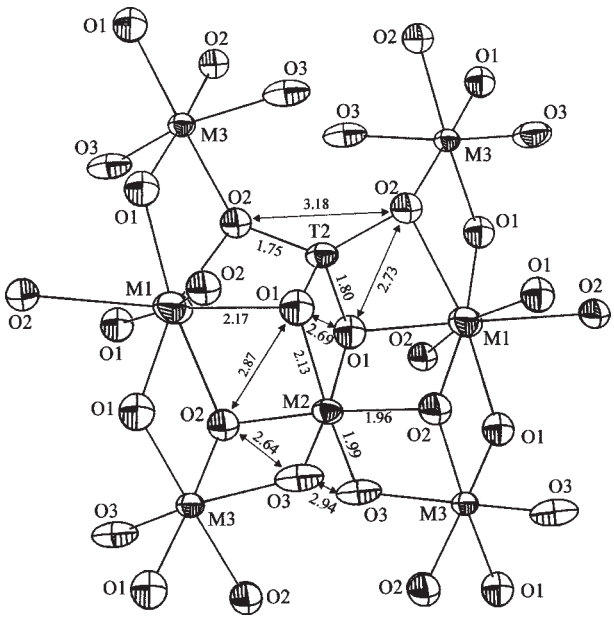

FIGURE 4. ORTEP representation of part of the tetragonal structure illustrating the distortions associated with the edge-sharing bewteen T2 and M2. Note the shortening of the O1···O1 shared edge. All distances are in Å. The displacement ellipsoids are drawn at 90% probability.

The garnet and tetragonal phases appear to be mutually exclusive in ternary germanate systems at normal pressure. For instance, the $CaO\text{-}Fe_2O_3\text{-}GeO_2$ system contains a garnet phase but no tetragonal phase while the reverse is true for the $MgO\text{-}Fe_2O_3\text{-}GeO_2$ system. On the other hand, both phases co-exist at 1 atm pressure in the quaternary $MgO\text{-}Fe_2O_3\text{-}Y_2O_3\text{-}GeO_2$ system. The tetragonal crystals were slightly larger than the gar-

TABLE 7. Fractional site occupancies for the known tetragonal phases $^{[VIII]}A^{[VI]}M_4^{[IV]}T_3O_{12}$

	T1	T2	M1 or A	M2	M3	Ref.
TAPP	Si	$Si_{0.92}Al_{0.08}$	$Mg_{0.76}Fe^{3+}_{0.19}$	$Al_{0.88}Cr_{0.08}Mn_{0.03}$	$Mg_{0.94}Fe^{2+}_{0.04}$	(1)
$Mg_{2.12}Fe_{3.17}Ge_{2.56}O_{12}$	Ge	$Ge_{0.78}Fe^{3+}_{0.22}$	$Mg_{0.52}Fe^{3+}_{33}$	$Mg_{0.22}Fe^{3+}_{0.78}$	$Mg_{0.56}Fe^{3+}_{0.44}$	(2)
$Ca_{0.32}Mg_{1.94}Fe_{3.12}Ge_{2.52}O_{12}$	Ge	$Ge_{0.76}Fe^{3+}_{0.24}$	$Ca_{0.33}Mg_{0.41}Fe^{3+}_{0.18}$	$Mg_{0.24}Fe^{3+}_{0.76}$	$Mg_{0.52}Fe^{3+}_{0.48}$	(2)
$Mg_{1.76}Y_{0.68}Fe_{3.37}Ge_{2.08}O_{12}$	Ge	$Ge_{0.54}Fe^{3+}_{0.46}$	$Y_{0.68}Mg_{0.21}$	$Mg_{0.26}Fe^{3+}_{0.74}$	$Mg_{0.51}Fe^{3+}_{0.49}$	(2)
$M_{4.5}As_3O_{12}$ (M = Co, Mg)	As	As	$M_{0.5}$	M	M	(3,4)
$NaMg_4V_3O_{12}$	V	V	Na	Mg	Mg	(5)
$Fe_{5.33}Ge_{2.67}O_{12}$	Ge	$Ge_{0.83}Fe^{3+}_{0.17}$	Fe^{2+}	Fe^{3+}	$Fe^{2+}_{0.83}Fe^{3+}_{0.17}$	(6)

Notes: (1) Sample 244B of Harris et al. 1997, (2) this work, (3) Krishnamachari and Calvo 1973, (4) Gopal et al. 1980, (5) Murashova et al. 1988, and (6) Modaressi et al. 1984.

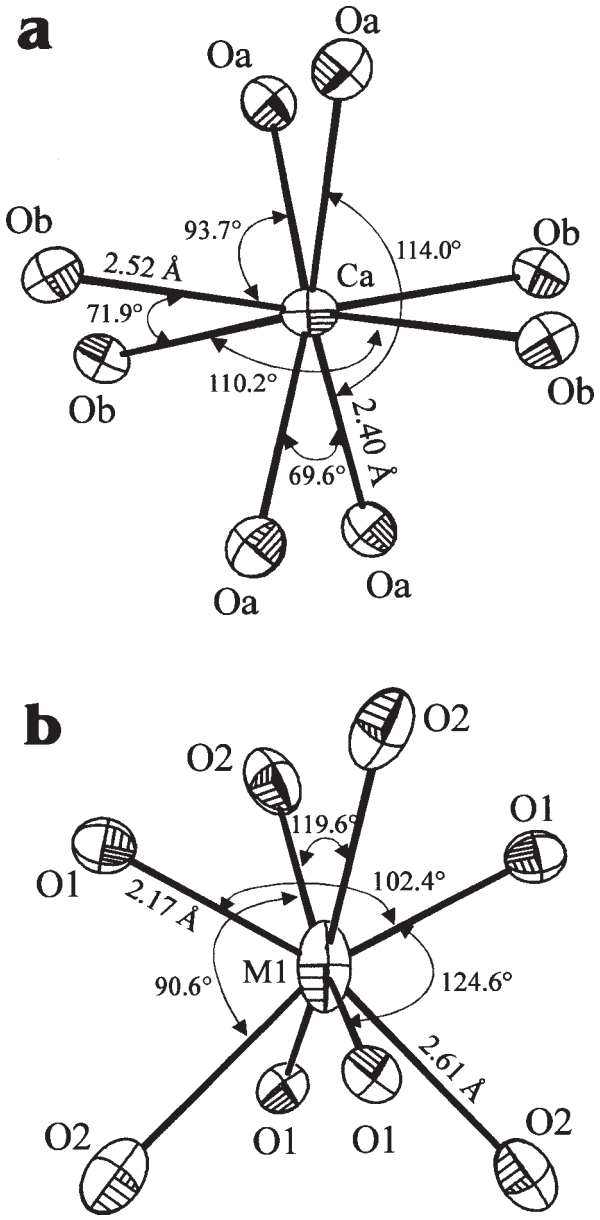

FIGURE 5. Geometries of the dodecahedral sites. (**a**) The garnet structure ($Ca_3Fe_2Ge_3O_{12}$). (**b**) The tetragonal structure ($Mg_{2.12}Fe_{3.17}Ge_{2.56}O_{12}$). Note the strong anisotropy of the M1 site in (**b**) associated with the long M1-O2 bonds.

net crystals, but both phases crystallized in large and approximately equal yields. The flux growth experiment in which these phases were recovered as single-crystals shows that they form with different compositions, mainly as a result of Fe and Y partitioning. The Fe^{3+} and Y^{3+} ions show a strong preference for the tetragonal phase and the garnet phase respectively, as demonstrated by the cation distributions: $^{VIII}(Y_{0.68}Mg_{0.21})^{VI}(Mg_{1.55}Fe_{2.45})^{IV}(Ge_{2.08}Fe_{0.92})O_{12}$ and $^{VIII}(Y_2Mg)^{VI}(Mg_{1.35}Fe_{0.56})^{IV}(Ge_{2.59}Fe_{0.41})O_{12}$ (Table 3). The Y^{3+} cations only occupy the dodecahedral sites of both structures and the larger proportion of these sites in garnet allows it to accommodate a larger Y-content. A similar partitioning can be expected for other large cations such as Ca^{2+} that would explain the low Ca-content found in the natural TAPP silicate (Harris et al. 1997).

ACKNOWLEDGMENTS

The diffraction data were measured by J. Britten (Department of Chemistry, McMaster University) and the microprobe analyses were carried out by C. Cermignani (Department of Geology, University of Toronto). The work was supported by a research grant to J.B. from the Canadian Natural Sciences and Engineering Research Council.

REFERENCES CITED

Barbier, J. (1989) New spinelloid phases in the $MgGa_2O_4$-Mg_2GeO_4 and $MgFe_2O_4$-Mg_2GeO_4 systems. European Journal of Mineralogy, 1, 39–46.

———(1998) Crystal structures of sapphirine and surinamite analogues in the MgO-Ga_2O_3-GeO_2 system. European Journal of Mineralogy, 10, 1283–1293.

———(1999) Tetragonal $Ni_{4.35}As_3O_{11.7}(OH)_{0.3}$. Acta Crystallographica, C55, CIF-access paper no. IUC9900080.

Brese, N.E. and O'Keeffe, M. (1991) Bond-valence parameters for solids. Acta Crystallographica, B47, 192–197.

Gopal, R., Rutherford, J. S., and Robertson, B. E. (1980) Closest packing in dense oxides: the structure of a polymorph of $Co_3(AsO_4)_2$. Journal of Solid State Chemistry, 32, 29–40.

Harris, J., Hutchison, M.T., Hursthouse, M., Light, M., and Harte, B. (1997) A new tetragonal silicate mineral ocurring as inclusions in lower-mantle diamonds. Nature, 387, 486–488.

Krishnamachari, N. and Calvo, C. (1973) Magnesium arsenate, $Mg_3As_2O_8$. Acta Crystallographica, B29, 2611–2613.

Lévy, D. and Barbier, J. (1999) Normal and inverse garnets: structures of $Ca_3Fe_2Ge_3O_{12}$, $Ca_3Y_2Ge_3O_{12}$ and $Mg_3Y_2Ge_3O_{12}$. Acta Crystallographica C55, 1611–1614.

Modaressi, A., Gerardin, R., Malaman, B., and Gleitzer, C. (1984) Structure et propriétés d'un germanate de fer de valence mixte $Fe_4Ge_2O_9$. Etude succincte de $Ge_xFe_{(3-x)}O_4$ ($x < 0.5$). Journal of Solid State Chemistry, 53, 22–34.

Murashova, E.V., Velikodnyi, Y.A., and Trunov, V.K. (1988) Crystal structure of $NaMg_4(VO_4)_3$. Journal of Structural Chemistry, 29, 648–650.

Siemens (1996) SAINT and SMART software, version 4.05, Siemens Energy And Automation Inc. Madison, WI.

Sheldrick, G.M. (1996) SADABS, Siemens Energy and Automation Inc. Madison, WI.

———(1997) SHELXL97; 97-2 edition, Göttingen, Germany.

Takayama, E., Kimizuka, N., Kato, K., Yamamura, H., and Haneda, H. (1981) The system GeO_2-FeO-Fe_2O_3 at 1000 °C. Journal of Solid State Chemistry, 38, 82–86.

Torres-Trevino, G., Lachowski, E.E., and West, A.R. (1986) A new lithium magnesium orthovanadate phase, $Li_{2x}Mg_{1.5-x}VO_4$ ($0.10<x<0.15$). Journal of Material Science Letters, 5, 615–616.

Vogt, R. and Müller-Buschbaum, H. (1991) Eine neue Phase mit Granatstuktur: $Ca_{10}Mg_5Cu_3V_{12}O_{48}$. Journal of Less-Common Metals, 171, 345–351.

MANUSCRIPT RECEIVED SEPTEMBER 7, 1999
MANUSCRIPT ACCEPTED FEBRUARY 29, 2000
PAPER HANDLED BY WILLAM BASSET